An ML Approach for Crosstalk-Aware Modulation Format Selection in SDM-EONs

Shrinivas Petale, Suresh Subramaniam

Department of Electrical and Computer Engineering, The George Washington University, Washington, DC, USA

{*srpetale, suresh*}*@gwu.edu*

Abstract—In space-division-multiplexed elastic optical networks (SDM-EONs), the routing, modulation, core, and spectrum assignment (RMCSA) problem is a critical lightpath resource assignment problem. Intercore-crosstalk (XT) between cores lowers the quality of parallel transmissions, and the RMCSA algorithm must ensure that XT restrictions are satisfied while optimizing network performance. There is a tradeoff between spectrum efficiency and XT tolerance - higher modulation formats are more efficient in terms of spectrum but are also less forgiving in terms of XT and allow fewer connections on adjacent cores on the overlapping spectrum. XT-aware RMCSA algorithms typically impose an upper limit or threshold on the number of lighted cores on the overlapped spectrum in order to ensure compliance with XT limits. In this paper, we offer a machine learning (ML)-assisted threshold optimization strategy that significantly enhances the performance of XT-aware RMCSA algorithms in terms of bandwidth blocking probability.

I. Introduction

Recent increases in bandwidth requirements for cloud-based services, 5G and 6G communications, high-resolution game streaming, and data center networks can be met via space division multiplexed elastic optical networks (SDM-EONs) [1]. Coherent optical transmission advancements have enabled fine-tuning of transmission parameters and an increase in spectral efficiency. SDM-EON provides parallel optical signal transmission over multicore fibers (MCFs) using distance-adaptive multicarrier transmission [2]. The quality of transmission (QoT) of signals carried by MCF, on the other hand, suffers due to intercore crosstalk (XT) between weakly coupled cores [3].

Owing to the small geometry of weakly coupled cores in MCF in SDM-EON, signal transmission does not mirror that of a multifiber connection, and the QoT of a signal on a spectrum slice worsens due to XT. As a result, it is critical to develop strategies for dealing with the effect of XT and to do so properly [4]. The choice of efficient modulation formats (MFs) has an effect on XT levels. Selecting a spectrally efficient MF (for e.g., PM-64QAM) saves spectrum but has a poor tolerance for XT and shorter transmission reaches (TRs). As a result, the resource assignment problem becomes more complex when multiple modulation formats are available. Many RMCSA algorithms fulfill XT restrictions by imposing a limit or threshold on the number of lit neighboring cores on overlapping spectrum [4], [5].

The maximum TR for a given MF can be obtained by considering the signal to noise ratio (SNR) in the form of accumulated XT to maintain the desired QoT. The XT accumulation for a lightpath increases with the number of *litcores* which is the number of Overlapping spectrum on

adjacent Cores (OsaCs), i.e., the number of existing lightpaths on adjacent cores that use overlapping spectrum. We assume that XT from only adjacent cores is significant in weakly coupled cores [6].

The decrease in SNR results in a decrease in TR, which means every litcore value corresponds to a different TR. Thus, MF selection can be modeled in terms of the number of litcores associated with the MFs. Error-vector magnitude (EVM) takes SNR into account and it degrades due to the penalties induced by in-band XT [7]. The TRs of each MF for different levels of XTs for different litcores can be obtained in terms of degradation of EVMs using approximated analytical modeling. There is a tradeoff between spectrum utilization and XT accumulation with respect to the selection of the MF.

In our recent work [8], we studied the improvement in performance due to careful selection of core-modulation format (MF)-spectrum combination. We discovered using extensive simulations that the proper selection of MF significantly improves the balance between spectrum utilization and XT accumulation, which results in decreased blocking. Recent advances in machine learning (ML) have enabled complicated problems in optical networks to be solved [9]. The underlying relationship between network features and output labels is discovered, and this information can then be used to construct network models. In this paper, we present a machine learning-aided strategy for learning such underlying relationships in order to improve MF selection and achieve a favorable tradeoff between spectrum usage and XT tolerance. Our technique is general in that it can be utilized with any XT-aware RMCSA algorithm.

The paper is organized as follows. The network model and problem statement are introduced in Sec. II. The proposed ML-aided approach is presented in Sec. III. Sec. IV presents simulation results and the last section concludes the work.

II. Network Model and Preliminaries

We now give the network model along with the transmission reach model. We also explain the problem description and illustrate how modifying the selection approach of MFs effect the resource assignment to connections.

A. Network Model and Problem Statement

We assume that the SDM-EON is equipped with coherent transceivers (TRXs) and works on a flexible grid with a granularity of 12.5 GHz. The TRXs support reprogrammable bit rates and a variety of MFs [6]. The TRXs operate at a constant baud rate of 28 GBaud, and each TRX transmits and receives

optical signals on a carrier with a total bandwidth occupying three frequency slices (FSs) (i.e., 37.5 GHz) [10]. If the desired bit rate is more than the capacity of a single TRX employing a specific MF, the request is carried by multiple optical carriers within a single superchannel (SCh). A 12.5 GHz guard band isolates each SCh from its neighbors. The nodes are connected through MCF-based optical links. Each fiber link is made up of identical MCFs with a specific core geometry in both directions. [1] Two generally accepted core geometries, three-core and seven-core, are investigated. We assume that the effect of XT impacts only adjacent/neighbor cores, and is negligible between non-adjacent cores. Each core in a three-core fiber, for example, contains two adjacent cores. Similarly, in a seven-core fiber, the outer cores are surrounded by three adjacent cores, while the center core is surrounded by six adjacent cores (see Figure 1). Additionally, spatial continuity is enforced, which implies that the same core is allocated to each lightpath on a route's MCF links. Lightpath requests arrive at a Poisson rate with an exponentially distributed mean holding time of unity (arbitrary units), while lightpath datarates are uniformly distributed over a predetermined range.

The mean XT experienced in a core of an MCF, denoted as XT_μ and shown in (1), can be obtained using an analytical model that uses coupled-power theory [6], [11]. Here, γ, h, and L are the litcores, a design parameter which represents the increase in XT per unit fiber length, and path length, respectively. γ is the number of OsaCs that are occupied by ongoing (parallel) transmissions, meaning, these adjacent cores are lit. The maximum TR (L_{max}) can be obtained using (2) where L_{span}, EVM_0, and EVM_{span} are the span length, EVM to attain target bit-error rate (BER), and EVM of the span, respectively [10]. The TR obtained with respect to the EVM ensures the BER of 3.8×10^{-3} for h of 3.15×10^{-9} and span length of 50km. The corresponding TR model is shown in [10].

$$XT_\mu = \frac{\gamma - \gamma\exp(-(\gamma+1)hL)}{1 + \gamma\exp(-(\gamma+1)hL)} \qquad (1)$$

$$L_{max} = L_{span} \left\lfloor \frac{\text{EVM}_0^2}{\text{EVM}_{span}^2} \right\rfloor \qquad (2)$$

The TR is a function of MF and γ. For a given γ, the TR of a higher MF, which is more spectrally efficient but more XT-sensitive, is lower than the TR of a lower MF. In addition, for a given MF, the TR decreases with increasing γ, as each increase in γ increases the XT accumulation. The MF selection for a lightpath can be controlled by specifying a maximum value of γ for each MF d, denoted as γ_{max}^d (explained through the example below), which serves as the threshold for selection of MFs. In other words, γ_{max}^d is the maximum number of OsaCs that are allowed to be occupied for the dth MF. This means that for a given MF d, no more than γ_{max}^d ($0 \le \gamma_{max}^d \le C-1$) OsaCs can be occupied by other existing/future connections during the holding time of the current connection if MF d

[1] In this paper, we assume that all the links have a single MCF in each direction, but the proposed work can be easily generalized for multiple fibers per link.

is chosen. Here, C denotes the total number of cores. This ensures that the XT will be capped in order to maintain the QoT. Using a higher γ_{max}^d allows more OsaCs to be occupied by other connections; however, this also means that the corresponding TR will be lower because of the higher potential XT. Thus, the set $\{\gamma_{max}^d : d = 1, \ldots, |D|\}$ (called *set of thresholds (ST)*) can be used to control the selection of MFs. For an arriving connection request, a resource allocation algorithm would choose the highest MF whose TR exceeds the path length of the connection; here, the TR depends on the ST. A candidate MF for assignment is defined below.

Definition II.1 (Candidate MF). Given a lightpath of length l, MF d is called as a candidate MF for assignment $\Longleftrightarrow$ the TR corresponding to γ_{max}^d, $T_d^\gamma \ge l$.

B. Illustrative Example

We now present an example to explain the influence of selection of γ_{max}^d on the tradeoff between spectrum usage and XT accumulation in the network. We will use Table I in [10] and Figure 1 for this illustration. We first show the effect of ST when all the thresholds are set to 0 on the occupancy of cores in spatial domain and corresponding occupancy of frequency slots in spectral domain. Later we explain the improvement by changing the ST.

Table I: Transmission reaches (in km) of MFs for different values of allowable lit core (γ) for a 7-core MCF for an average XT per span of -40dB (from Table I in [10]).

γ (Lit-cores)	Modulation Formats ($|D| = 5$, $f_d \in D$)				
	PM-QPSK	PM-8QAM	PM-16QAM	PM-32QAM	PM-64QAM
0	5200	2050	1100	550	250
1	4650	1850	1000	500	250
2	4200	1650	900	450	200
3	3850	1500	800	400	200
4	3550	1400	750	400	150
5	3300	1300	700	350	150
6	3050	1200	650	300	150

For a connection arrival, the path length of the shortest path (SP) between source and destination nodes is used to get the MF as per Definition II.1. For this example, we consider the selection pattern of MF and corresponding γ^d as shown in our work [8]. Readers may refer the Algorithm 1 in [8] for better understanding of selection of MF and γ, and how it represents the spectrum requirement and allowed occupancy of the OsaCs. The only difference will be that in this example first fit policy is imposed to determine the highest MF. The TRs (T_d^γ) for different values of γ for each MF for the network model explained above is given in Table I, and are used to select the MF. Later the spectrum and core are selected. Let us assume that $D = \{\text{PM-32QAM } (d = 4), \text{PM-64QAM } (d = 5)\}$ for this example. The links are equipped with 7-core fibers with cores 1 to 6 at the periphery and the core 7 is at the center. Suppose a 320 Gbps connection arrives on route r. The spectrum requirements for this connection using PM-64QAM and PM-32QAM (including guardband (GB)) are 4 FSs and 7 FSs, respectively. Suppose γ_{max}^4 and γ_{max}^5 are set
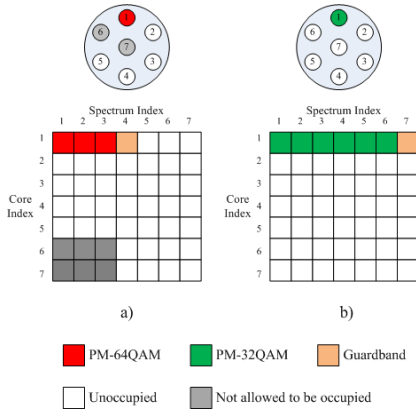
Figure 1: Change in spectrum utilization for two different selections of MFs.

to 0. Suppose the length of the SP is 250 km and that the spectrum on all the links on this SP is unoccupied. Here, PM-64QAM with $\gamma^5 = 1$ will be selected since ($l =$) 250km is less than or equal to the TR, at $\gamma^5 = 1$, ($T_5^1 =$) 250km. Here, $\gamma^5 = 1$ means if PM-64QAM is chosen for this connection, only one OsaC among the OsaCs on cores 2, 6, and 7 is allowed to be occupied by other connections during this connection's holding time in order to maintain the QoT. Suppose that the OsaCs on cores 6 and 7 are not allowed to be occupied as shown in Figure 1a. In this case, the spectrum of 4 FSs on core 1, and 3 FSs each on cores 6 and 7 need to be reserved for this connection, for a total of 10 FSs. The other MFs will not be considered as we have found the first MF suitable for this connection, and thus this connection will be established on core 1 using FSs 1 to 4. Remember that we take the occupancy of OsaCs into consideration during the selection process. For example, assume that the FSs 1 to 4 are already occupied by another ongoing connections on any of the two cores, let's say cores 6 and 7, then this MF can't be selected since to maintain the QoT of PM-64QAM for this connection we need the OsaC atleast one core out of the three adjacent cores to be free. There are other conditions for assignment which are defined in Definition V.1 in [8].

Now suppose that the γ_{max}^5 is changed from 0 to 2. In this case, T_5^2 (= 200 km) is less than the path length of 250 km, and therefore PM-64QAM cannot be selected on this SP. The next MF PM-32QAM is then considered. The TR at $\gamma^4 = 6$ ($T_4^6 = 300$ km) is greater than or equal to the path length of 250 km. Thus we can use PM-32QAM for assignment. $\gamma^4 = 6$ implies that there is no limitation on OsaCs and the same spectrum on all the three adjacent cores will be allowed to be occupied by future connections as shown in Figure 1b. Thus the reserved spectrum is only 7 FSs as shown in Figure 1b. It is evident from this example that the choice of ST can improve the selection process of MF.

III. MACHINE LEARNING-AIDED LITCORE THRESHOLD SELECTION

We now present a novel approach for selecting optimal litcore thresholds that is aided by machine learning. This approach can be used by *any* RMCSA algorithm that meets XT constraints using litcore thresholds. In this section, we discuss the prerequisites for the machine learning model (MLM) and its working principle. Recall that D denotes the set of MFs and γ_{max}^d denotes the litcore threshold for the dth MF. The first step is to collect samples of sets of thresholds (STs), followed by training the MLM. Let the optimal value of γ_{max}^d be denoted by γ_*^d. The steps involved in machine learning-aided threshold optimization to obtain γ_*^d for all MFs using MLM are illustrated in Figure 2 and explained below.

A. Data Generation

First, the problem is defined to select the network parameters in the Problem Definition stage. The data is then fed to the data generation model. In the Synthetic Data Generation stage, a small sample of random STs is generated and the corresponding BBPs are obtained for a given RMCSA algorithm through simulation. To generate a single value of BBP from an ST, dynamic network operations must be simulated which also involves the selection of MFs as per Definition II.1. Because simulating performance for all possible STs would take an inordinate amount of time, we let the MLM learn the relationship between ST and BBP and select the optimal ST. Furthermore, network telemetry is difficult and getting precise network data requires separate expenditure in a real network [12]. Therefore, we generate several hundreds of ST samples and then obtain the corresponding BBP values through simulation. These STs are then fed into the MLM, which develops an understanding of the relationship and can then predict the BBP of the remaining STs. The MLM's training and prediction times are negligible in comparison to the total computation time required to generate the BBP for each sample. Additionally, the MLM can be easily modified by altering the hyperparameters, which increases the flexibility of the learning process. The difference between predicted and actual BBP values for STs with known BBPs is used to tune and calibrate the MLM for precise predictions.

Let S_i^γ and B_i^γ denote the ith ST ($|S_i^\gamma| = |D|$) and corresponding BBP. Each ST is used to generate the filtered TR model to select the MF. The selection of route, MF, core, and spectrum is done using the RMCSA algorithm of choice. It is very unlikely to have the optimal ST present in the small set of randomly selected STs used for training. Hence, the load for the training data generation is chosen such that the BBP values are somewhat higher than desired ($10^{-2} to 10^{-1}$) so that the MLM can discriminate between various STs (as lower loads may give a BBP of 0 for several STs).

B. Machine Learning Model and Threshold Selection Technique

We use a deep-neural network (DNN) as the MLM. The optimal γ^d is denoted as γ_*^d and optimal ST is denoted as S_*^γ ($=\{\gamma_*^1, \gamma_*^2, \ldots, \gamma_*^{|D|}\}$). The feature-label samples are used to train the DNN, which then predicts the S_*^γ. The feature-label samples are used to train the MLM. The MLM seeks statistical relationships and learns more effectively when the dataset is pre-processed prior to feeding it to the MLM. The second
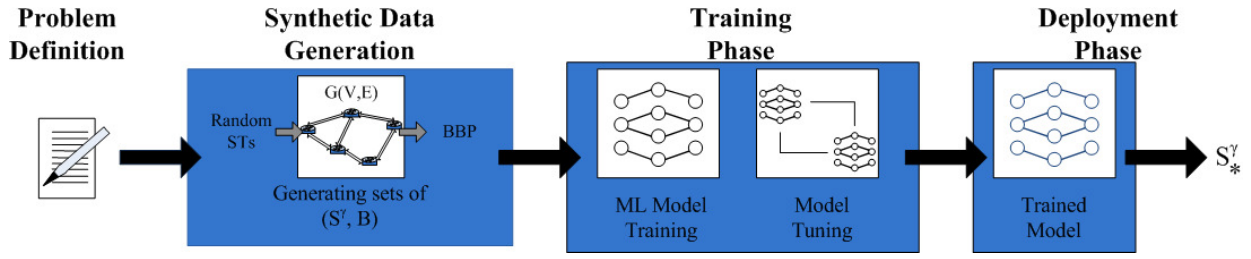
Figure 2: Machine learning approach for selection of optimal ST.

step as illustrated in Figure 2, which is the Synthetic Data Generation phase, produces the STs (S_i^γ) and corresponding BBPs (B_i^γ) which then acts as the input to the MLM. The details of the steps involved in training the model (Training Phase (Figure 2)) and optimizing the STs (Deployment Phase (Figure 2)) are given in Algorithm 1.

Figure 3: Performance of DNN with respect to (e-η).

Algorithm 1 ML-Aided Optimization Model

Input: STs S_i^γ and corresponding B_i^γ

Output: S_*^γ

1: Select the desired features
2: Get F_t and F_t', and P_t and P_t'
3: Get F_t^s and $F_t^{s'}$ by scaling F_t and F_t' using the mean and standard deviation of F_t
4: Train and Tune the MLM by choosing hyperparameters to get as low validation loss as possible using F_t^s and P_t
5: Get the desired hyperparameters by regularization
6: Train the model with obtained hyperparameters on F_t^s and P_t
7: Use GridSearchCV() and trained model to get S_*^γ

In Line 1 of Algorithm 1, the features are processed. Each feature value is checked to determine its contribution in the label. In other words, if a change to a feature has no effect on the label, the change is noted and the feature is discarded from the learning process. In our case, we observed that altering the values of γ_{max}^d has an effect on the BBP.

The selected features are then statistically processed in the last phases of data preprocessing. To begin, the entire dataset is separated into training and testing subsets (Line 2). Generally, 80% of samples are used for training and 20% for testing. A portion of training dataset (around 80%) is used for training the model and the remaining for validation. This step is essential so as to track whether the model is overfitting or not. The training dataset's features and labels are denoted as F_t and P_t, respectively. The testing dataset's features and labels are denoted as F_t' and P_t'. Both F_t and F_t' are scaled (or normalized) to F_t^s and $F_t^{s'}$ using F_t's mean and standard deviation (Line 3).

The model is trained using the default hyperparameters and the training and validation loss are monitored (Line 4). We use k-fold cross validation (kCV) to get the errors to check the fit of the model. The training and tuning are repeated until the best hyperparameters are obtained using F_t^s and P_t (Line 5). We use regularization as discussed briefly in the next subsection. We observed that the MLM with tuned hyperparametes performs at least 20% better than the MLM with default hyperparameters. Finally, the tuned hyperparameters
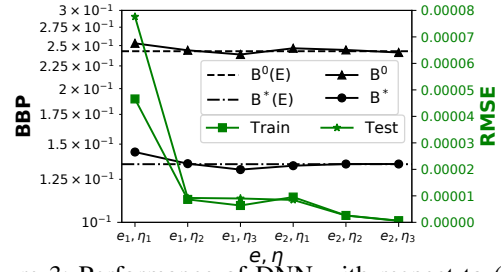
are used to train the model, which discovers the fundamental relationship between STs and the BBPs (Lines 6). The trained MLM, employing the gridsearch process, returns the set of γ_*^d denoted by S_*^γ (Line 7).

During our extensive experiments with the variable sizes of feature sets, we observed that the relationship between the γ_{max}^d and BBP is not linear. We experimented with a variety of MLMs for regression and discovered that the DNN regression model performs the best. Hence, the findings for DNN MLM are reported in this study.

C. Tuning the Machine Learning Model

During training, the DNN can suffer from overfitting, wherein it works well with the known data but poorly with unknown data. We use a two-step process to avoid this as mentioned in Lines 4 and 5 in Algorithm 1. The first is to split a portion of the training data into validation dataset to monitor the validation loss. The second step is the use of callbacks. Callbacks are set to stop the learning process at a lower epoch when the performance of DNN does not improve for e epochs.

The DNN is comprised of input, hidden, and output layers. The output layer is set to *Regression* mode and has a single node. The number of epochs and DNN parameters, such as the number and type of neuronal layers and the number of neurons comprising each layer, affect the performance of DNN. The proper selection of the parameters can be done using *Pruning*, which is out of scope of this paper, and we therefore include experimental values that follow $n_h = T/\alpha(n_i + n_o)$ where, n_h, T, n_i and n_o are the number neurons in hidden layer(s), total samples, input nodes, and output nodes, respectively, and α is a scaling factor. The BBP (on left y-axis), and root mean square error (RMSE) value corresponding to the training and testing (on right y-axis) with respect to the number of epochs (e) and set of neurons per hidden layer (η) is shown in Figure 3. The results are obtained for first-fit RSA (xtFF) (explained in Sec. IV) with complete dataset of all samples divided into

training (80%) and testing data (20%). The validation dataset is 20% of the training data and no callbacks are set ($e=0$). $B^0(E)$ and B^0 denote experimental and predicted BBP when all thresholds are set to 0, and $B^*(E)$ and B^* denote the experimental and predicted BBP corresponding to the optimal thresholds. Let e_i denote the ith value of number of epochs. Let η_i denote the set of neurons per hidden layer (n_h) for i hidden layers. Here, $e_1=10$, $e_2=50$, $\eta_1=\{16\}$, $\eta_2=\{16,16\}$, $\eta_3=\{16,32,16\}$. It can be seen that DNN with η_3 (denser version) predicts the B^0 and B^* better than DNN with η_1 and η_2. It also offers lower prediction error with respect to the training and testing datasets.

Once the epochs and DNN parameters are selected, the training and testing datasets are standardized using mean and variance of training dataset. Here, the mean is subtracted from each feature which is then scaled to unit variance. The trained DNN is then used with the GridSearchCV procedure to get S_*^γ in the Deployment phase. The MLM uses the pre-calculated TRs corresponding to different γ values. Thus the MLM works as the *generalized model* which can be used with any TR model and RSA.

IV. Simulation Results

We now present simulation results for a range of scenarios in which we compare the chosen RMCSA with and without machine learning-assisted optimization. We employ two topologies, namely generic German (DT) and European (EURO) [8]. A spectrum of 4 THz is considered on each core with a slice width of 12.5 GHz, or 320 FSs ($S = 320$). Poisson connection arrival process with exponential holding times of mean one (arbitrary time unit) is assumed. The Erlang loads were chosen to maintain a BBP range of approximately 10^{-5} to 10^{-1}. 100,000 requests are generated in each trial, excluding 10,000 warm-up requests to let the network reach steady state. Each experiment yields 95 percent confidence intervals after ten trials. The datarates are uniformly distributed between 40 and 400 Gbps with a 40 Gbps granularity. Three SPs ($K = 3$) are considered for each s-d pair. The set of assignable modulation formats is denoted by $D = \{f_1, f_2, \ldots, f_{|D|}\}$, where f_1 is the lowest modulation format and $f_{|D|}$ is the highest modulation format. We assume five modulation schemes in this article: PM-QPSK (f_1), PM-8QAM, PM-16QAM, PM-32QAM, and PM-64QAM (f_5). The transmission reach (i.e., the maximum length which can be traversed while maintaining the desired QoT) is dependent on both the MF of the lightpath and the status of overlapping spectrum on adjacent cores (OsaCs). TR models for each MF with an average crosstalk of -40 dB between two adjacent cores after a single span propagation and a TRX operating at 28 GBaud and a span length of 50 km are taken from [10]. Only 100 and 200 data samples are generated for the case of $C = 3$ and $C = 7$, respectively, and 80% of these are used for training and the remainder for validation. To obtain assessment scores, the kCV employs $k = 5$ folds.

For this study, the RMCSAs XT-aware first fit (xtFF), xtFF with modulation selection (xtFM), and P-XT [6] are chosen.

Table II: ML based $S_*^\gamma=\{\gamma_*^1, \gamma_*^2, \gamma_*^3, \gamma_*^4, \gamma_*^5\}$ for DT topology

RSA	$C = 3$	$C = 7$
xtFF	{ 1, 0, 2, 2, 2 }	{ 3, 0, 3, 6, 6 }
xtFM	{ 0, 0, 2, 2, 2 }	{ 6, 5, 3, 3, 3 }
P-XT [6]	{ 0, 0, 0, 2, 2 }	{ 0, 6, 3, 2, 2 }

Table III: ML based $S_*^\gamma=\{\gamma_*^1, \gamma_*^2, \gamma_*^3, \gamma_*^4, \gamma_*^5\}$ for EURO topology.

RSA	$C = 3$	$C = 7$
xtFF	{ 1, 1, 2, 1, 1 }	{ 1, 3, 5, 6, 3 }
xtFM	{ 1, 2, 2, 0, 2 }	{ 0, 3, 3, 5, 6 }
P-XT [6]	{ 0, 1, 2, 2, 2 }	{ 6, 3, 6, 5, 1 }

In xtFF and P-XT, based on the path length, only the first fit highest MF is selected and checked for assignment. If the spectrum and the core are not available, i.e., don't satisfy the XT constraint, the connection is blocked. In xtFM, the above step is repeated to get all the MFs for which the spectrum and core are available, and the highest MF is chosen. Readers may refer [8] and [6] to understand the XT-aware approach to select path, MF, spectrum, and core.

The S_*^γ for all the algorithms for both core geometries are shown in Table II for DT topology and in Table III for EURO topology; which is then used to select MFs as per Definition II.1. The utilized epochs out of 50 due to callbacks for xtFF, xtFM and P-XT are 29, 21, and 25 for $C = 3$, and 24, 18, and 17 for $C = 7$ for DT topology. The comparison between RSA and their ML-aided version for $C = 3$ and $C = 7$ for DT and EURO topologies is shown in Figure 4. The corresponding utilization of MFs is shown in Figure 5. It is clear the ML-aided versions of all the RSAs outperform the unaided RSAs by up to three orders of magnitude. The main reason for this to happen can be seen in the distribution of MFs. In all the cases, the selection of higher MFs is slightly reduced and the selection of lower MFs is slightly increased. It becomes possible because the MLM learns that the balance can be made between the selection MFs in terms of spectrum utilization and XT accummulation by choosing optimal γ_*^d. We observed that by using S_*^γ, the non-ML assisted variant never chooses a lower MF such as PM-8QAM in case of $C = 7$ in DT topology (Figure 4b) but the ML-assisted version brings it in by limiting the selection of higher MFs i.e. PM-64QAM (Figure 5b). Higher MFs require less spectrum for the connection, but due to their XT sensitivities the OsaCs are blocked. On the other hand, lower MFs require more spectrum for the connection but also block less spectrum on OsaCs due to lower XT sensitivity. The MLM successfully balances this tradeoff and achieves excellent performance. The selection of lower MFs is higher in EURO than DT because the path lengths of EURO topology are longer than that of DT. We also observed that in some of the cases either the non-ML assisted versions or the ML-assisted versions of xtFF and xtFM performs almost the same. The reason for this is the similar selection pattern of MFs. Here the reason for blocking can be either the unavailability of the spectrum (for e.g. due to fragmentation) or due to QoT constraints (e.g. spectrum being blocked by ongoing connections as shown in Figure 1).

The performance of ML aided versions of RMCSAs can easily be improved further by choosing more samples for

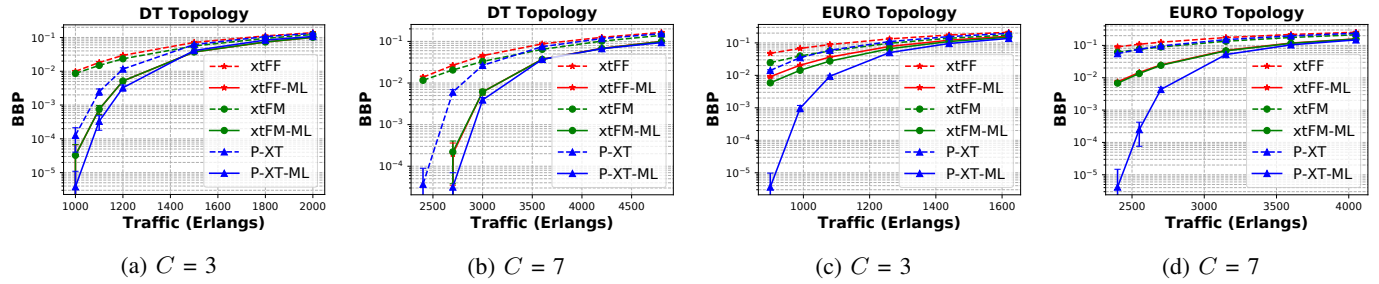(a) $C = 3$ (b) $C = 7$ (c) $C = 3$ (d) $C = 7$

Figure 4: Variation in BBP for all RMCSAs and their ML-aided versions with respect to the traffic for DT topology (Figure 4a, 4b) and EURO topology (Figure 4c, 4d).

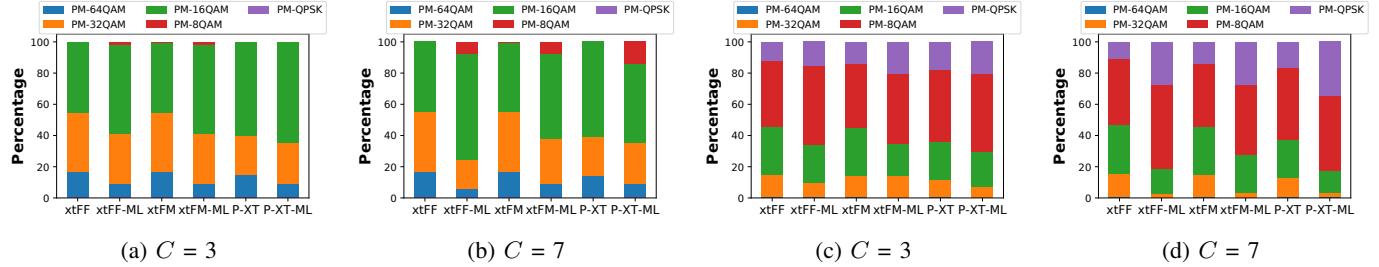(a) $C = 3$ (b) $C = 7$ (c) $C = 3$ (d) $C = 7$

Figure 5: Distribution of MFs for all RMCSAs and their ML-aided versions with respect to the traffic for DT topology (Figure 5a, 5b) and EURO topology (Figure 5c, 5d).

training. Based on extensive simulations, we observed that number of samples, and number of hidden layers and neurons per hidden layer are inversely proportional. As it is desired to get the optimal ST with as less STs as possible and availability of the computation power, denser DNN are used in this paper.

V. CONCLUSION

For space division multiplexed elastic optical networks, we studied crosstalk-aware RMCSA algorithms. Depending on the modulation type chosen, a tradeoff exists between spectrum usage and inter-core crosstalk (XT) accumulation. Many RMCSA techniques meet XT requirements by imposing a constraint on the number of litcores on overlapped spectrum. We suggested a machine learning-assisted strategy in this study for optimizing the thresholds used to govern the selection of MFs. The technique is applicable to any RMCSA allocation mechanism that constrains the number of litcores to satisfy XT requirements. We evaluated the performance of several existing RMCSA algorithms and their ML-aided variants and demonstrated that the latter decrease the bandwidth blocking probability of dynamic connection requests by up to three orders of magnitude for different combinations of topologies and types of cores. A very intriguing observation is that the ML-aided variant of the worst performing baseline method outperforms the best performing algorithm that does not use ML to optimize the threshold.

REFERENCES

[1] B. Shariati, D. Klonidis, I. Tomkos, D. Marom, M. Blau, S. Ben-Ezra, M. Gerola, D. Siracusa, J. Macdonald, N. Psaila, *et al.*, "Realizing spectrally-spatially flexible optical networks," *IEEE Photon, Society Newsletter*, pp. 4–9, 2017.

[2] Y. Awaji, J. Sakaguchi, B. J. Puttnam, R. S. Luís, J. M. D. Mendinueta, W. Klaus, and N. Wada, "High-capacity transmission over multi-core fibers," *Optical Fiber Technology*, vol. 35, pp. 100–107, 2017.

[3] M. Klinkowski, P. Lechowicz, and K. Walkowiak, "Survey of resource allocation schemes and algorithms in spectrally-spatially flexible optical networking," *Optical Switching and Networking*, vol. 27, pp. 58–78, 2018.

[4] M. Yang, Y. Zhang, and Q. Wu, "Routing, spectrum, and core assignment in sdm-eons with mcf: node-arc ilp/milp methods and an efficient xt-aware heuristic algorithm," *Journal of Optical Communications and Networking*, vol. 10, no. 3, pp. 195–208, 2018.

[5] K. Walkowiak, A. Wlodarczyk, and M. Klinkowski, "Effective worst-case crosstalk estimation for dynamic translucent sdm elastic optical networks," in *ICC 2019-2019 IEEE International Conference on Communications (ICC)*, pp. 1–7, IEEE, 2019.

[6] M. Klinkowski and G. Zalewski, "Dynamic crosstalk-aware lightpath provisioning in spectrally-spatially flexible optical networks," *IEEE/OSA Journal of Optical Communications and Networking*, vol. 11, no. 5, pp. 213–225, 2019.

[7] P. Martelli and P. Boffi, "Crosstalk-induced penalty in coherent space-division multiplexing transmission," in *2018 20th International Conference on Transparent Optical Networks (ICTON)*, pp. 1–4, IEEE, 2018.

[8] S. Petale, J. Zhao, and S. Subramaniam, "Tridental resource assignment algorithm for spectrally-spatially flexible optical networks," in *ICC 2021-2021 IEEE International Conference on Communications (ICC)*, pp. 1–7, IEEE, 2021.

[9] F. Musumeci, C. Rottondi, A. Nag, I. Macaluso, D. Zibar, M. Ruffini, and M. Tornatore, "An overview on application of machine learning techniques in optical networks," *IEEE Communications Surveys & Tutorials*, vol. 21, no. 2, pp. 1383–1408, 2018.

[10] C. Rottondi, P. Martelli, P. Boffi, L. Barletta, and M. Tornatore, "Crosstalk-aware core and spectrum assignment in a multicore optical link with flexible grid," *IEEE Transactions on Communications*, vol. 67, no. 3, pp. 2144–2156, 2018.

[11] M. Klinkowski, P. Ksieniewicz, M. Jaworski, G. Zalewski, and K. Walkowiak, "Machine learning assisted optimization of dynamic crosstalk-aware spectrally-spatially flexible optical networks," *Journal of Lightwave Technology*, vol. 38, no. 7, pp. 1625–1635, 2020.

[12] M. Ibrahimi, H. Abdollahi, C. Rottondi, A. Giusti, A. Ferrari, V. Curri, and M. Tornatore, "Machine learning regression for qot estimation of unestablished lightpaths," *Journal of Optical Communications and Networking*, vol. 13, no. 4, pp. B92–B101, 2021.